Interfacial Nanosphere Lithography toward Ag_2S–Ag Heterostructured Nanobowl Arrays with Effective Resistance Switching and Enhanced Photoresponses

*Yang Li, Xiaozhou Ye, Yurong Ma, and Limin Qi**

Heterostructures of semiconductors and noble metals are attracting increasing interest because of their unique properties arising from the combined properties and synergistic interactions of the metallic and semiconducting components, as well as versatile applications in electronic and optical devices, electrocatalysis and photocatalysis, solar energy harvesting, and biotechnology.[1–5] In particular, considerable efforts have been devoted to the controlled fabrication of hybrid nanostructures comprising Ag_2S and noble metals, such as composite nanoparticles of Ag_2S and various noble metals,[3] core-shell Au@Ag_2S nanoparticles,[6] hollow-solid Ag_2S–Ag nanocomposites,[2,7] porous Ag_2S–Ag hybrid nanotubes,[4] periodic Ag_2S-AuAg heterostructured nanowires,[5] Ag_2S–Ag hybrid nanoprisms,[8,9] and Ag_2S–Au hybrid nanoframes.[10] Such Ag_2S-noble metal heterostructures have demonstrated potential applications in electrocatlysis,[3] photocatalytic degradation[4,7a] and water splitting,[5,10] bacterial deactivation,[2,9] and biosensing.[8] Moreover, as typical ionic conductor/metal hybrid nanostructures, Ag_2S–Ag nanowire heterostructures have shown promising applications in resistance switching and nonvolatile memory devices.[11–13] Nevertheless, most of the aforementioned Ag_2S–noble metal heterostructures are discrete hybrid nanostructures, and the subsequent integration into large-scale, uniform devices are required for certain applications. It remains a great challenge to develop facile and rational strategies for the large-scale fabrication of ordered arrays of Ag_2S–noble metal hybrid nanostructures.

The nanosphere lithography technique based on monolayer colloidal crystals (MCCs) has been demonstrated to be a facile, inexpensive, efficient, and flexible approach toward two-dimensionally (2D) patterned nanostructures with distinct properties and promising applications in a variety of technologically important areas.[14–17] Particularly, nanosphere lithography at the gas–liquid interface, which employs floating MCCs at solution surface as the template for interfacial deposition, provides a facile and efficient route toward free-standing patterned thin films, such as Ag_2S nanonets[18] and Ag[19] or ZnS[20] nanobowl arrays. While a variety of physical processes-aided nanosphere lithography methods have been developed for the fabrication of periodic nanostructure arrays including heterogeneous array of bimetal particles,[21] it is difficult to achieve semiconductor-metal heterostructure arrays with tunable architectures by these methods. Therefore, the morphology-controlled fabrication of 2D ordered nanoarrays of uniform semiconductor-metal heterostructures through nanosphere lithography remains challenging. Herein, we report a facile, two-step interfacial nanosphere lithography strategy for the controllable fabrication of large-area Ag_2S–Ag heterostructured nanobowl arrays consisting of Ag_2S nanonets lying on Ag nanobowl arrays. The unique Ag_2S–Ag heterostructured nanobowl arrays exhibited effective resistance switching behaviors and enhanced photoresponses, showing potential applications in both electric devices and photocatalysis.

As shown in **Figure 1**, a two-step interfacial nanosphere lithography method was used to fabricate the Ag_2S–Ag heterostructured nanobowl arrays. First, a hexagonal-close-packed (hcp) MCC film made of polystyrene (PS) spheres (600 nm in diameter) was transferred onto the surface of aqueous $AgNO_3$ solution. Then, H_2S gas was introduced into the system, and a piece of Ag_2S nanonet film was obtained after the preferential deposition of Ag_2S at the gas–liquid interface. Due to capillary force, the solution would fill the triangular interstices among three adjacent PS spheres, resulting in a continuous Ag_2S nanonet film. Subsequently, N_2H_4/NH_3 gas mixture diffused into the system, leading to the reduction of Ag^+ ions and the preferential deposition of metallic Ag at the bottom of each PS spheres. Hence, Ag_2S–Ag heterostructured nanobowl arrays consisting of Ag_2S nanonets lying above the tangent-point plane and Ag nanobowl arrays enclosing the lower part of the MCC template were produced. It may be noted that cavities would form at the connection regions of neighboring spheres. After removal of the MCC template, 2D ordered arrays of Ag_2S–Ag heterostructured nanobowls consisting of connected Ag_2S rings

Y. Li, Dr. X. Ye, Prof. Y. Ma, Prof. L. Qi
Beijing National Laboratory for Molecular Sciences (BNLMS)
State Key Laboratory for Structural Chemistry of Unstable and Stable Species
College of Chemistry
Peking University
Beijing 100871, P. R. China
E-mail: liminqi@pku.edu.cn

DOI: 10.1002/smll.201402078

www.MaterialsViews.com

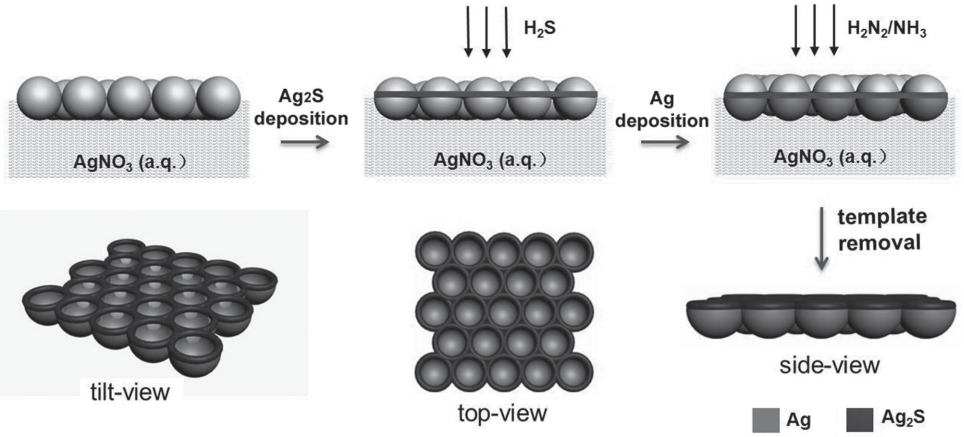

Figure 1. Schematic illustration of the fabrication of Ag_2S–Ag heterostructured nanobowl arrays by two-step nanosphere lithography at the gas–liquid interface.

lying on the edge of Ag bowls with some cavities on the lateral walls were obtained.

Following the reported fabrication procedures for Ag_2S nanonets[18] and Ag nanobowl arrays[19] by nanosphere lithography at the gas–liquid interface with slight modifications, uniform Ag_2S nanonets and Ag nanobowl arrays can be readily prepared separately. For the Ag_2S deposition induced by H_2S diffusion, the nucleation tended to occur at the gas–liquid interface. The Ag_2S particles deposited above the tangent point plane of PS spheres and grew toward the spheres into gas phase, resulting in the formation of a uniform Ag_2S-MCC composite film (Figure S1a,b, Supporting Information). After removal of the MCC template, a free-standing Ag_2S nanonet film was harvested (Figure S1c,d, Supporting Information). Unlike the Ag_2S nanonets, the Ag deposition induced by diffusion of the N_2H_4/NH_3 gas mixture would preferentially occur at the liquid-solid interface, leading to the formation of large-area, continuous Ag nanobowl arrays (Figure S2, Supporting Information). It may be noted that cavities existed in the lateral bowl walls at the connection regions of neighboring PS spheres.

Considering that Ag_2S nanonets and Ag nanobowl arrays tended to form independently by preferential deposition at two different regions, uniform Ag_2S–Ag heterostructured nanobowl arrays could be readily prepared by combining the two deposition processes via a two-step interfacial nanosphere lithography strategy (Figure 1). After successive deposition of Ag_2S nanonets and Ag nanobowl arrays, a uniform Ag_2S–Ag-MCC composite film was obtained, as shown in the scanning electron microscopy (SEM) images presented in **Figure 2**a,b. The hexagonally packed PS spheres and the regular Ag_2S nanonet located at upper layer could be seen from the top view (Figure 2a), which reveals that the hole diameter is around 350 nm and the bar width is about 150 nm. The side view (Figure 2b) demonstrates the existence of both Ag_2S nanonets and Ag nanobowl arrays, which are well-collected. After removal of the MCC template, uniform Ag_2S–Ag heterostructured nanobowl arrays about several cm^2 in area were obtained (Figure S3, Supporting Information). As shown in Figure 2c, the heterostructured nanobowl arrays maintained their original morphology, showing a hexagonally ordered structure. All the bowls had a relatively smooth, hemispherical bottom, indicating a good replication of the PS spheres (Figure 2d). The tilt view proves the existence of the cavities in the lateral bowl walls at the connection regions of neighboring PS spheres (Figure 2e). Figure 2f indicates that the thickness of the flat Ag_2S net is ~60 nm, while the bottom wall of the Ag nanobowls is much thicker (~200 nm).

The Ag_2S–Ag heterostructured nanobowl arrays were further characterized by using energy dispersive X-ray spectroscopy (EDS) to obtain information about the distribution of each chemical composition. Figure 2g shows periodic variations in element distribution for both Ag and S along the line scanning through hole centers, with S reaching the maximum at the net regions and Ag reaching the maximum at the hole centers, in good agreement with the Ag_2S–Ag heterostructured nanobowl structure. The EDS spectra in spot-scanning mode (Figure 2h) clearly shows that both S and Ag could be detected for the Ag_2S nanonet region (spot 1) whereas only Ag was detected in hole centers where Ag nanobowls were located (spot 2). All these results confirm the formation of the Ag_2S–Ag heterostructured nanobowl arrays consisting of connected Ag_2S rings lying on the edge of Ag bowls.

It is known that Ag_2S is a typical ionic conductor, and the Ag_2S–Ag heterojunction may be employed to make functional resistance switches.[11–13] Accordingly, an electrical transfer and switching device based on the Ag_2S–Ag heterostructured nanobowl arrays was built. To obtain this device, a piece of fluoride-doped tin oxide (FTO) glass was used as the baseplate to pick up the heterostructured nanobowl arrays. Then, another piece of FTO was put on the Ag_2S–Ag heterostructures-covered FTO with an insulative tape covering the edge to avoid the direct contact of the two FTO electrodes (Figure S4, Supporting Information). The device configuration (FTO/Ag/Ag_2S/FTO) is schematically shown in **Figure 3**a, and the measured current-voltage (*I–V*) curve is shown in Figure 3b, which exhibited a characteristic reversible switching behavior between "ON" and "OFF" conductance states under the cyclic voltammograms. When the initial voltage applied on the FTO electrode beside the Ag nanobowl arrays was highly positive (~2 V), Ag filaments formed

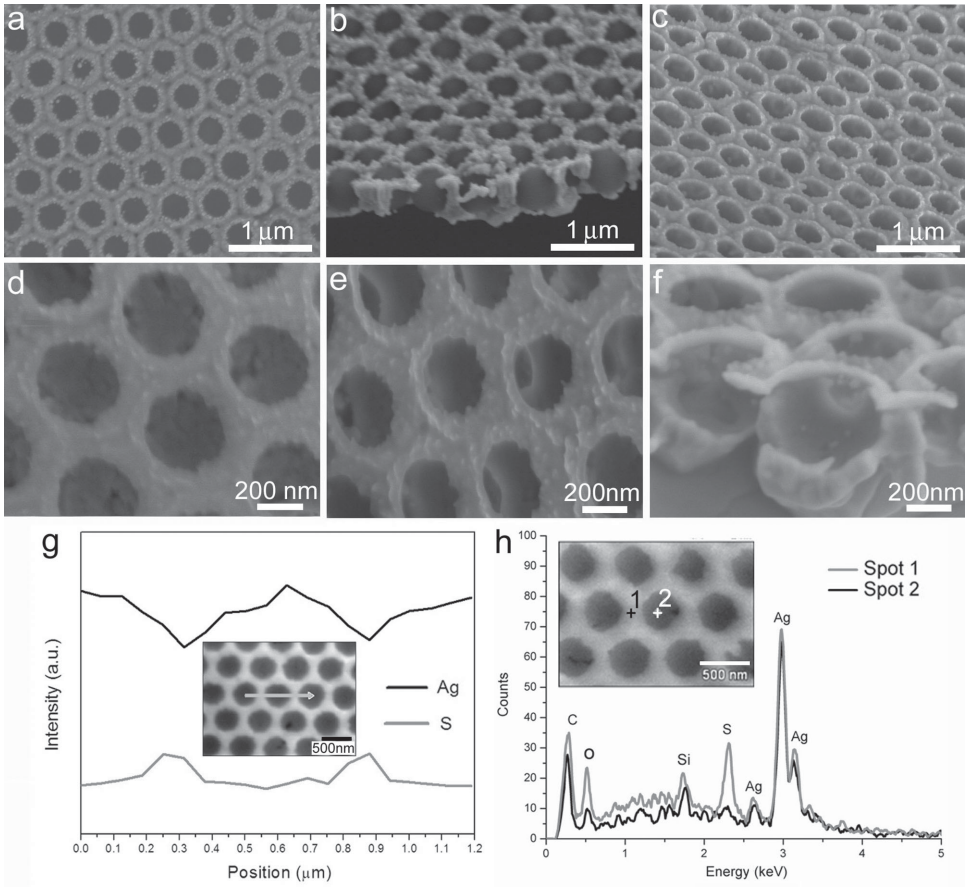

Figure 2. SEM images of Ag_2S–Ag heterostructured nanobowl arrays before (a,b) and after (c–f) removal of MCC template. EDS analysis results: (g) elemental profiles of line scanning, (h) EDS spectra of two selected spots.

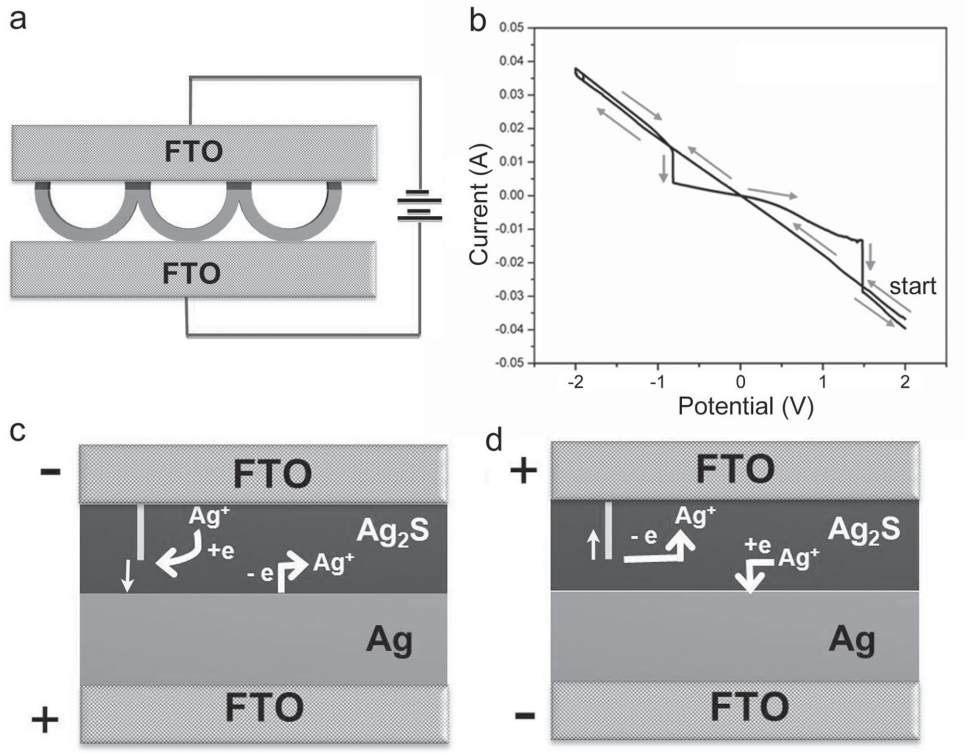

Figure 3. Schematic structure (a) and *I–V* curve (b) of FTO/Ag/Ag_2S/FTO device made of the heterostructured nanobowl arrays. (c,d) Schematic illustration of the operating mechanism.

www.MaterialsViews.com

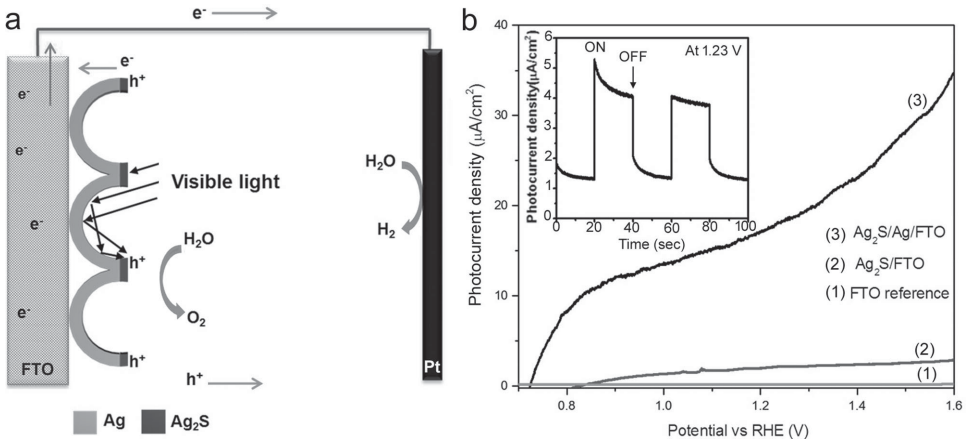

Figure 4. a) Schematic diagram of electron/hole transport for water splitting in an Ag_2S/Ag/ FTO photoelectrochemcial cell (PEC) using the Ag/Ag_2S/FTO as the photoanode. b) Linear sweep voltammograms curves under visible light illumination for Ag_2S/Ag/FTO and Ag_2S/FTO PECs together with blank FTO. The inset shows the corresponding amperometric *I–t* curve under light switching on and off at an applied potential of 1.23 V vs RHE.

quickly to bridge the FTO electrode and the Ag nanobowl, leading to the device in its ON state with a low resistance (~56 Ω) due to the conductive Ag bridges (Figure 3c). When scanning the voltage from 2 V to 0 V, the voltage on the Ag nanobowl arrays side was kept positive and the device was in its ON state, thus a linear change was obtained in the *I–V* curve. Subsequently, the voltage turned negative, and the voltage on the Ag nanobowl arrays side became negative, and the Ag filaments formed at the Ag/Ag_2S interface were dissolved gradually (Figure 3d). However, since the dissolving of the Ag filaments would take some time, the electrode still kept in its ON state when the voltage was swept from 0 V to –2 V. When scanning the voltage back from –2 V, there was an abrupt current drop at -0.8 V. This result indicates that the Ag filament was dissolved to a certain degree and the conductive bridge was broken, resulting in the device in its OFF state with a very high resistance (~214 Ω) owing to the low conductivity of Ag_2S. The resistance was further increased up to ~3000 Ω when the voltage approached 0 V, which corresponding to a maximum R_{OFF}/R_{ON} ratio ~54. With the voltage turning positive again, the Ag filament would gradually form and the resistance became lower. When the voltage reached 1.5 V, another abrupt current change occurred, indicating the transition from OFF to ON state again.

Similar devices were reported for an individual Ag_2S–Ag nanowire heterostructure,[11] hybrid Ag_2S–Ag nanowires,[13] and physically contacted Ag_2S–Ag nanofiber bundles.[12] In the current situation, the large-area, uniform Ag_2S–Ag heterostructured nanobowl arrays have been demonstrated to exhibit effective resistance switching behaviors. The thin Ag_2S nanonets with a uniform thickness (~60 nm) showed good contact with the Ag nanobowls, leading to a highly reversible switching behavior. Furthermore, the precise adjustment of weight ratio of Ag_2S and Ag in the composite films or the thickness of the Ag_2S nanonets and Ag nanobowls may allow for further tuning of the resistance and thus the device properties. Hence, the obtained Ag_2S–Ag heterostructured nanobowl arrays may provide a useful platform for the reproducible fabrication of electrical switching and memory devices with new configuration and tunable properties.

Recently, the research on the desirable photoelectrode materials for photocatalytic water splitting has attracted intensive interest,[22] and the potential applications of Ag_2S-nobel metal hybrid nanostructures in this area have been explored.[5,10] Therefore, the Ag_2S–Ag heterostructured nanobowl arrays collected on an FTO slide were directly used as a photoanode of photoelectrochemical cell (PEC) for water splitting as a proof-of-concept application, as illustrated in **Figure 4**a. Upon visible light illumination, the electron-hole pairs were generated in Ag_2S nanonets. The applied potential in the PEC would drive the photo-generated electrons to move towards the Pt electrode, where the reduction of H_2O to H_2 would happen. The holes left on the Ag_2S surfaces would oxidize H_2O to O_2. The unique structure of the Ag_2S–Ag heterostructured nanobowl arrays would show remarkable advantages for the photocatalytic water splitting. First, the Ag nanobowl arrays between Ag_2S nanonets and FTO are able to act as an electron sink to facilitate the photogenerated-electrons transfer from Ag_2S to the Pt electrode,[5,10] thus improving the charge separation. Second, the nanobowl array structure could considerably enhance light harvesting by multiple scattering of light inside the bowls. The measured linear sweep voltammograms curves of the Ag_2S–Ag heterostructured nanobowl arrays, the pure Ag_2S nanonets, and the blank FTO slide are shown in Figure 4b. As a reference, the Ag_2S/FTO PEC has a photocurrent of 2.1 μA cm^{-2} at the thermodynamic water oxidation potential, i.e.,1.23 V vs reversible hydrogen electrode (RHE), while the blank FTO slide has a photocurrent density of merely 0.2 μA cm^{-2}, indicating that the pure Ag_2S nanonets had a certain degree of photocatalytic activity. Notably, the Ag_2S/Ag/FTO PEC exhibits a photocurrent density of 17.9 μA cm^{-2} at 1.23 V vs RHE, which corresponds to an increase to ~8.5 times of the photocurrent density for the Ag_2S/FTO PEC. This remarkable enhanced current density could be largely related to the enhanced charge separation and light harvesting attributed to the Ag nanobowl arrays attached to the bottom of the Ag_2S nanonets. Namely, the Ag nanobowl arrays bridging Ag_2S nanonets and FTO are able to act as an electron sink to facilitate the transfer of the photogenerated electrons

from Ag_2S to the Pt electrode and hence improve the charge separation; moreover, the nanobowl array structure can lead to multiple scattering of light inside the bowls, thus considerably enhancing the absorption of light by the outer Ag_2S nanonet layer. Therefore, the unique nanobowl array structure has the advantage of enhancing light harvesting and it may be reasonably expected that the photocatalytic activity of the Ag_2S–Ag heterostructured nanobowl arrays could be adjusted by changing the pore size of the nanobowl array due to the modification of the performance of light harvesting. Compared with the reported Ag_2S-nobel metal hybrid nanostructures,[5,10] the current Ag_2S–Ag heterostructured nanobowl arrays have a distinct two-layer structure, which may be beneficial to both charge separation and light absorption, thus showing potential applications in photocatalysis. For giving a further sense of the photoactivity of this heterostructure, the photocurrent under AM 1.5G solar light simulator was measured, which shows that a photocurrent density of ~170 μA cm^{-2} at 1.23 V vs RHE can be achieved for the Ag_2S–Ag heterostructured nanobowl arrays (Figure S5, Supporting Information).

Furthermore, the Ag_2S/Ag/FTO PEC exhibits effective sensitivity to visible light, as displayed by the corresponding amperimetric photocurrent density-time (*J*–*t*) cycles (inset of Figure 4b). It may be noted that when the light was suddenly switched on at a constant applied potential of 1.23 V vs RHE, the photocurrent density was around 4 μA cm^{-2}, which is significantly lower than the photocurrent density obtained from the linear sweep voltammograms curves, i.e., 17.9 μA cm^{-2}. The measurement of the *J*–*t* curves from different Ag_2S/Ag/FTO PECs demonstrated the reproducibility of this phenomenon. Actually, similar decrease from the photocurrent related to the linear sweep voltammograms curves to the transient photocurrent related to the *J*-*t* curves has been previously observed for the Ag_2S-AuAg heterostructured nanowires[5] and Ag_2S-Au hybrid nanoframes.[10] Although the exact mechanism of this phenomenon remains unclear at the present time, it could be attributed to the fast recombination of holes trapped at surface states with electrons from the conduction band in this Ag_2S-based system. It has been documented that such a recombination of holes and electrons usually results in the photocurrent decay with time.[23] Therefore, a fast hole-electron recombination in this system combined with a relatively slow diffusion of reactive species would lead to fast decay of the transient photocurrent or a significant decrease in the apparent initial photocurrent obtained from the *J*–*t* curves.

In summary, we achieved the facile fabrication of unique Ag_2S–Ag heterostructured nanobowl arrays for the first time by two-step nanosphere lithography at the gas–liquid interface. The successive interfacial deposition of Ag_2S and Ag against the MCC template allowed for the controllable fabrication of highly ordered, heterostructured nanobowl arrays consisting of Ag_2S nanonets lying on Ag nanobowl arrays. The heterostructured nanobowl arrays exhibited effective resistance switching behaviors, thus showing the potential application in electronic switches and memory devices. Meanwhile, the heterostructured nanobowl arrays exhibited enhanced photocatalytic activity owing to their unique structure when they were used as a photoanode for water splitting. Furthermore, this work may open new avenues toward facile and rational synthesis of large-area ordered arrays of semiconductor-noble metal hybrid nanostructures with multifunctions.

Experimental Section

Materials: Monodisperse polystyrene (PS) spheres ~600 nm in diameter were purchased from Tianjin Baseline ChromTech Research Centre. Thioacetamide (TAA) was obtained from Sinopharm Chemical Reagent Co., Ltd. Silver nitrate was purchased from Beijing Chemical Works. Strong aqua ammonia was purchased from Beijing Tongguang Fine Chemical Company. Hydrazine aqueous solution (85 wt%) was purchased from Sinopharm Chemical Reagent Co., Ltd. Fluoride-doped tin oxide (FTO) glass was obtained from Nippon Sheet Glass Co., Ltd.

Characterization: The morphology and composition of the samples were characterized by scanning electron microscopy (SEM, Hitachi FE-S4800, 5~10 kV or Nova Nano 430, 5~10 kV) and energy-disperse X-ray spectroscopy (EDS, Nova Nano 430, 5~10 kV).

Assembly of the MCC Template at the Solution Surface: First, the monolayer colloidal crystal film was fabricated on a silicon or glass substrate using a method developed at our lab.[24] In brief, 20–25 μL water/ethanol dispersion containing monodisperse PS colloidal spheres was dropped onto the top surface of a 1 cm × 1 cm piece of glass surrounded by water located at the mid bottom of a Petri dish. The dispersion spread freely on the water surface until it covered nearly the whole surface area, resulting in a colorful MCC film. A few microliters of SDS solution (2 wt%) was then dropped onto the water surface to lower the surface tension, which packed the MCC film on water surface closely. Then, the MCC film was picked up by a silicon or glass plate and dehydrated naturally in air.

Fabrication of Ag_2S–Ag Heterostructured Nanobowl Arrays: A two-step, interfacial nanosphere lithography method was used to fabricate the Ag_2S–Ag heterostructured nanobowl arrays. It included the successive fabrication of Ag_2S nanonets and Ag nanobowl arrays via nanosphere lithography at the gas–liquid interface.

Step 1: For the fabrication of the heterostructured arrays, the synthesis of Ag_2S nanonets was carried out at first following the reported procedure[18] with slight modifications. Typically, the MCC film on 1 cm × 1 cm silicon plate was first transferred onto the surface of 10 mM $AgNO_3$ aqueous reactant solution by inserting the loaded silicon plate into the solution with an inclining angle. Then, the vessel containing $AgNO_3$ aqueous solution with a piece of MCC film floating on the solution surface was placed in a closed desiccator where one vial containing 5 mL of 0.5 M TAA acted as the source for H_2S gas to initiate the interfacial reaction with silver ions. Here, the TAA solution was used instead of TAA powder for controlling the synthesis more precisely. All these experiments were carried at room temperature. After reaction for 48 hours, the resultant Ag_2S-MCC composite films were picked up from the solution surface by certain substrates.

Step 2: The Ag_2S-MCC composite films were transferred onto the surface of 10 mM $AgNO_3$ aqueous reactant by the same method in step 1. Then, the vessel containing $AgNO_3$ aqueous solution with a piece of Ag_2S-MCC composite films floating on

the solution surface was placed in a closed desiccator where one vial containing 3 mL of strong aqua ammonia and 7 mL of hydrazine aqueous solution (85 wt%) acted as the source for gaseous reductant. After reaction for 24 hours, the Ag films formed at the lower part of the PS spheres were continuous and robust to external force. The resultant Ag_2S–Ag-MCC composite films were picked up from the solution surface by certain substrates, and the PS spheres were dissolved with toluene, resulting in the formation of Ag_2S–Ag heterostructured nanobowl arrays. Based on the measurement of the weights of the Ag_2S nanonets and the Ag_2S–Ag heterostructured nanobowl arrays, the weight ratio of Ag and Ag_2S in the heterostructure was estimated to be ~ 3.6:1.

Fabrication of the FTO/Ag/Ag_2S/FTO Device: The FTO slide was used to pick up the Ag_2S–Ag-MCC composite films from the solution surface. It may be noted that for a better conductance between the FTO slide and the Ag_2S–Ag heterostructured nanobowl arrays, a multilayer film of pure Ag nanobowl arrays (typically 4~5 layers) was usually packed onto the the FTO slide before the Ag_2S–Ag composite films were picked up. After dehydrated naturally in air, two parts of the device were fixed with a clincher. For the measurements of the resistance switching properties, four samples were studied to ensure the reproducibility.

Water Splitting: The experiment for water splitting was carried out by measuring the photocurrent correlated with the water dissociation. To measure the photocurrent, an electrochemical workstation (CHI 660C) with a three-electrode configuration, where Ag_2S/Ag/FTO photoanode, Ag/AgCl electrode and Pt electrode were used as the working, reference and counter electrodes, respectively, was employed in 1 M NaOH solution (pH = 13.6). A 300 W Xe lamp with a cutoff filter of 420 nm (PLS-SXE 300C) was used to provide the visible illumination on Ag_2S/Ag/FTO. For the measurements of the photoelectrochemical properties, six samples were studied to ensure the reproducibility. For comparison purposes, the photocurrent under solar light simulator was also measured with simulated sunlight from the 300 W Xe lamp using a filter (AM 1.5G) with a measured intensity of 1 sun (100 mW cm^{-2}) at the sample face.

Supporting Information

Supporting Information is available online from the Wiley Online Library or from the author.

Acknowledgements

This work was supported by NSFC (grant nos. 21173010, 21073005, and 51121091) and MOST (grant no. 2013CB932601).

[1] a) R. Jiang, B. Li, C. Fang, J. Wang, *Adv. Mater.* **2014**, *26*, 5274–5309; b) S. T. Kochuveedu, Y. H. Jang, D. H. Kim, *Chem. Soc. Rev.* **2013**, *42*, 8467–8493; c) X. Huang, Z. Zeng, S. Bao, M. Wang, X. Qi, Z. Fan, H. Zhang, *Nat. Commun.* **2013**, *4*, 1444; d) Z. Zeng, C. Tan, X. Huang, S. Bao, H. Zhang, *Energ. Environ. Sci.* **2014**, *7*, 797–803; e) Z. Yin, J. Zhu, Q. He, X. Cao, C. Tan, H. Chen,Q. Yan, H. Zhang, *Adv. Energy Mater.* **2014**, *4*, 1300574; f) T.-H. Yang, L.-D. Huang, Y.-W. Harn, C.-C. Lin, J.-K. Chang, C. Wu, J.-M. Wu, *Small* **2013**, *9*, 3169–3182.
[2] M. Pang, J. Hu, H. C. Zeng, *J. Am. Chem. Soc.* **2010**, *132*, 10771–10785.
[3] J. Yang, J. Y. Ying, *Angew. Chem. Int. Ed.* **2011**, *50*, 4637–4643.
[4] W. Yang, L. Zhang, Y. Hu, Y. Zhong, H. B. Wu, X. W. Lou, *Angew. Chem. Int. Ed.* **2012**, *51*, 11501–11504.
[5] X. Hong, Z. Yin, Z. Fan, Y. Tay, J. Chen, Y. Du, C. Xue, H. Chen, H. Zhang, *Small* **2014**, *10*, 479–482.
[6] J. Yang, J. Y. Ying, *Chem. Commun.* **2009**, 3187–3189.
[7] a) H. Liu, F. Ye, H. Cao, G. Ji, J. Y. Lee, J. Yang, *Nanoscale* **2013**, *5*, 6901–6907; b) J.-N. Gao, H.-B. Zhao, L.-M. Qi, *Acta Phys. -Chim. Sin.* **2012**, *28*, 2487–2492.
[8] B. Liu, Z. Ma, *Small* **2011**, *7*, 1587–1592.
[9] S. Xiong, B. Xi, K. Zhang, Y. Chen, J. Jiang, J. Hu, H. C. Zeng, *Sci. Rep.* **2013**, *3*, 2177.
[10] L. Xu, Z. Yin, S. Cao, Z. Fan, X. Zhang, H. Zhang, C. Xue, *Chem. Eur. J.* **2014**, *20*, 2742–2745.
[11] C. Liang, K. Terabe, T. Hasegawa, M. Aono, *Nanotechnology* **2007**, *18*, 485202.
[12] H. Wang, L. Qi, *Adv. Funct. Mater.* **2008**, *18*, 1249–1256.
[13] G. R. Bourret, R. B. Lennox, *Nanoscale* **2011**, *3*, 1838–1844.
[14] J. Zhang, Y. Li, X. Zhang, B. Yang, *Adv. Mater.* **2010**, *22*, 4249–4269.
[15] X. Ye, L. Qi, *Nano Today* **2011**, *6*, 608–631.
[16] Y. Li, N. Koshizaki, W. Cai, *Coord. Chem. Rev.* **2011**, *255*, 357–373.
[17] Y. Li, G. Duan, G. Liu, W. Cai, *Chem. Soc. Rev.* **2013**, *42*, 3614–3627.
[18] C. Li, G. Hong, L. Qi, *Chem. Mater.* **2010**, *22*, 476–481.
[19] G. Hong, C. Li, L. Qi, *Adv. Funct. Mater.* **2010**, *20*, 3774–3783.
[20] X. Ye, Y. Li, J. Dong, J. Xiao, Y. Ma, L. Qi, *J. Mater. Chem. C* **2013**, *1*, 6112–6119.
[21] J. Wang, F. Zhou, G. Duan, Y. Li, G. Liu, F. Su, W. Cai, *RSC Adv.* **2014**, *4*, 8758–8763.
[22] a) Z. Li, W. Luo, M. Zhang, J. Feng, Z. Zou, *Energy Environ. Sci.* **2013**, *6*, 347–370; b) F. E. Osterloh, *Chem. Soc. Rev.* **2013**, *42*, 2294–2320.
[23] a) H. M. Chen, C. K. Chen, R.-S. Liu, L. Zhang, J. Zhang, D. P. Wilkinson, *Chem. Soc. Rev.* **2012**, *41*, 5654–5671; b) J.-S. Yang, W.-P. Liao, J.-J. Wu, *ACS Appl. Mater. Interfaces* **2013**, *5*, 7425–7431.
[24] C. Li, G. Hong, P. Wang, D. Yu, L. Qi, *Chem. Mater.* **2009**, *21*, 891–897.

Received: July 15, 2014
Revised: August 19, 2014
Published online: September 18, 2014